

Heat transfer and thermal stress analysis in fluid-structure coupled field



Ming-Jian Li, Jun-Hua Pan, Ming-Jiu Ni, Nian-Mei Zhang*

School of Physics, University of Chinese Academy of Sciences, Beijing 100190, China

HIGHLIGHTS

- We use FVM and FEM to investigate FCI structural safety considering heat transfer and FSI effects.
- Higher convective heat transfer coefficient is beneficial for the FCI structural safety without much affect to bulk flow temperature.
- Smaller FCI thermal conductivity can better prevent heat leakage into helium, yet will increase FCI temperature gradient and thermal stress.
- Three-dimensional simulation on conjugate heat transfer in a fluid-structure coupled field was carried out.

ARTICLE INFO

Article history:

Received 20 June 2014

Received in revised form

1 August 2014

Accepted 20 September 2014

Available online 5 October 2014

Keywords:

Fluid channel insert

Fluid-structure interaction

Heat transfer

Thermal stress

ABSTRACT

In this work, three-dimensional simulation on conjugate heat transfer in a fluid-structure coupled field was carried out. The structure considered is from the dual-coolant lithium-lead (DCLL) blanket, which is the key technology of International Thermo-nuclear Experimental Reactor (ITER). The model was developed based on finite element-finite volume method and was employed to investigate mechanical behaviours of Flow Channel Insert (FCI) and heat transfer in the blanket under nuclear reaction. Temperature distribution, thermal deformation and thermal stresses were calculated in this work, and the effects of thermal conductivity, convection heat transfer coefficient and flow velocity were analyzed. Results show that temperature gradients and thermal stresses of FCI decrease when FCI has better heat conductivity. Higher convection heat transfer coefficient will result in lower temperature, thermal deformations and stresses in FCI. Analysis in this work could be a theoretical basis of blanket optimization.

© 2014 Elsevier Ltd. All rights reserved.

1. Introduction

Nuclear fusion would be a very promising energy source in the future. Many scholars in US, EU, Russia, China, etc have been working together in International Thermo-nuclear Experimental Reactor (ITER) project. In the dual-coolant lithium-lead (DCLL) blanket module concept, flow channel insert (FCI) acts as electrical and thermal insulator between the hot PbLi fluid and the load-bearing structural steel wall [1–3]. FCI is usually made of silicon carbide composites. S. Smolentsev et al., developed code for analysis of magneto-hydrodynamics (MHD) pressure drop in a liquid metal blanket [4,5]. Numerical simulations of MHD flow and heat transfer in poloidal metal channel of DCLL blanket with a SiC composites flow channel insert were carried out in UCLA [6,7]. In

China, Z. Xu et al., studied the influence of MHD effects in blanket with the FCI. The experimental results implied that the FCI with pressure equalization slot (PES) or pressure equalization holes (PEH) greatly affected the velocity distribution of bulk flow in blanket [8,9]. W. Wang and Y. Wu analyzed MHD effects and thermal stresses of DFL with numerical method [10,11]. Results indicated that magnetic field would make the velocity profile of liquid metal much more complicated, and led to different temperature distribution.

Despite much work about MHD and heat transfer analysis, less has been discussed about structural safety of FCI considering its material property under multi-physics fields. In this paper, numerical simulation on thermal fluid-structure coupled field was carried out. Thermal deformation and stress states in FCI were obtained by using the CFD and FEM code. The relationship between the maximum displacement and stress in FCI and physical characteristics of FCI were analyzed. The influences of FCI material characteristics and fluid flowing on heat transfer and temperature field were investigated.

* Corresponding author.

E-mail addresses: nmzhang@ucas.ac.cn, nianmeizhang@yahoo.com (N.-M. Zhang).

2. Mathematical model

This work studied temperature and thermal stress field of flow channel insert (FCI) in multi-physics coupled field using U.S. DEMO DCLL design as a prototype. The sketch of a typical blanket channel with FCI is shown in Fig. 1. FCI seats inside the blanket channel, forming a thin gap in the channel. Both the gap and space inside FCI are filled with flowing Pb–17Li driven by the same pressure head. In what follows, we refer to flow inside FCI as “bulk flow” and that in the space between the FCI and ferritic wall as “gap flow”. Flow and heat transfer process in the blanket is shown in Fig. 2. The average entrance speed is 0.06 m/s, and inlet temperature is 733 K. Helium temperature outside ferritic wall is 673 K. Along the flow direction, heat from core area of blanket is transferred through FCI and ferritic wall to outside helium. FCI immersed in metal fluid which would lead to thermal stress. In this model, x , y and z coordinate direction are set to be radial, toroidal and poloidal directions, respectively. The dimension and parameters of reference blanket are summarized in Table 1. To be noted, parameters in different designs are varied and still under optimization, in this case, parameters in a typical model are applied [6,7].

3. Governing equations and solution method

PbLi metal fluid in bulk flow and gap flow is considered as incompressible fluid and is governed by N–S Equation (1), continuity Equation (2), and energy Equation (3).

$$\frac{\partial \vec{v}}{\partial t} + (\vec{v} \cdot \nabla) \vec{v} = -\frac{1}{\rho} \nabla p + \nu \nabla^2 \vec{v} \quad (1)$$

$$\nabla \cdot \vec{v} = 0 \quad (2)$$

$$\rho C_v \left(\frac{\partial T}{\partial t} + \vec{v} \cdot \nabla T \right) = k \nabla^2 T \quad (3)$$

where, \vec{v} , p , T are velocity vector of fluid, kinetic pressure and temperature, respectively. ν , k , C_v , ρ refer to the fluid viscosity, thermal conductivity, specific heat capacity and fluid density.

FCI and ferritic wall meet heat conduction Equation (4).

$$k \nabla^2 T = 0 \quad (4)$$

The inlet end of fluid is set with a constant velocity and temperature. Pressure boundary condition is applied for outlet end.

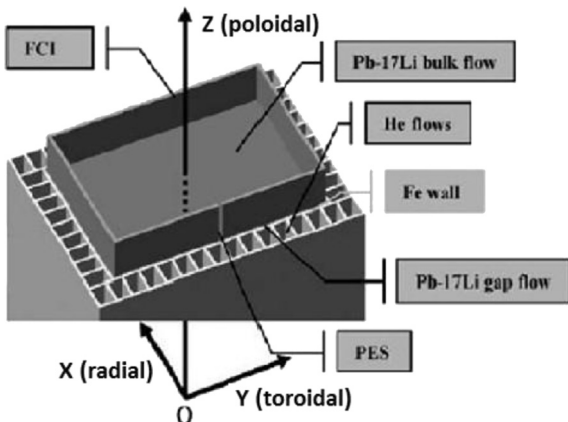


Fig. 1. Geometry of DCLL blanket [6].

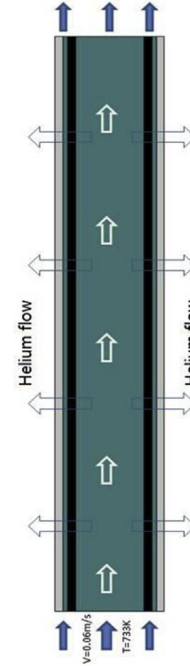


Fig. 2. Sketch of flow and heat transfer in DCLL.

Outside the structure, convective heat transfer between steel wall and helium is assumed, the third boundary condition is satisfied here.

$$q'' = h(T_{fe} - T_{he}) \quad (5)$$

where, h means the convective heat transfer coefficient. T_{fe} and T_{he} express the temperature of steel wall and helium as a coolant.

Following conjugated heat transfer conditions (6) and (7) should be satisfied on the fluid-structure interaction surfaces, i.e., interface between bulk flow and FCI, FCI and gap flow, gap flow and ferritic wall.

$$T_s = T_f \quad (6)$$

$$q_s = q_f \quad (7)$$

Here, T , q indicate temperature and heat flow. And the subscripts s , f signify solid and fluid, respectively.

Geometric equation for small deformation in FCI is

$$\varepsilon_{ij} = \frac{1}{2}(u_{i,j} + u_{j,i}) + \alpha \Delta T \delta_{ij} \quad (i, j = x, y, z) \quad (8)$$

Table 1

Typical blanket channel parameter and boundary conditions.

Poloidal length	2 m
FCI channel inner sizes	0.3 m * 0.2 m (toroidal * radial)
FCI thickness	0.005 m
Gap width	0.002 m
Ferritic wall thickness	0.005 m
Pb–17Li mean flow velocity	0.06 m/s
Helium temperature	400 °C
Inlet Pb–17Li temperature	460 °C
Heat transfer coefficient in helium	4000 W/m ² K

Table 2
Material properties.

Pb–17Li density	9151	kg/m ³
Pb–17Li dynamic viscosity coefficient	0.001	Pa s
Pb–17Li thermal conductivity	16	W/m K
Pb–17Li specific heat capacity	187	J/(kg K)
Steel wall thermal conductivity	30	W/m K
SiC thermal conductivity	2	W/m K
SiC elastic modulus	2 × 10 ¹¹	Pa
SiC Poisson's ratio	0.2	1
FCI thermal expansion coefficient	3.3 × 10 ⁻⁶	K ⁻¹
Heat transfer coefficient in helium	4000	W/m ² K
Helium temperature	673	K
SiC bending strength	3.46 × 10 ⁸	Pa
SiC tensile strength	3.26 × 10 ⁸	Pa
SiC compressive strength	4.05 × 10 ⁸	Pa

where, ϵ_{ij} represents strain tensor, u_i represents displacement vector and α is thermal expansion coefficient of SiC. ΔT denotes the variation of temperature in FCI. δ function meets

$$\delta_{ij} = \begin{cases} 1 & i = j \\ 0 & i \neq j \end{cases} \quad (9)$$

FCI is made of silicon carbide composites. As described by Y. Katoh [12], SiC is the candidate material for FCI, because of its good electrical and heat insulating characteristic. And its constitutive relation meet generalized Hooke law in elastic state. Constitutive equation for linear material is

$$\sigma_{ij} = 2G\epsilon_{ij} + \lambda\theta\delta_{ij} \quad (10)$$

where, σ_{ij} is defined as stress tensor. G is shear modulus and $\lambda = E\nu/(1 + \nu)(1 - 2\nu)$ is Lamé constant. $\theta = \epsilon_{ii}$ is volumetric strain (Table 2).

Sequential method, which is widely used to simulate the fluid-structure interaction, was employed to investigate temperature distribution and thermal deformation of FCI in a thermal-fluid-structure coupling field. Fig. 3 indicates the calculating process of steady fluid-structure interaction (FSI). Initially, conjugate heat transfer in both fluid and structure were analyzed. Then the surface temperature of FCI was transmitted to structure as boundary conditions. Finally, finite element analysis code was employed to solve deformations and stresses in FCI. The code based on Openfoam was applied to solve the fluid part and Ansys code was used to solve the solid part. A consistent and conservative scheme was used in the MHD calculation, and validation has been carried out in previous work [13].

4. Results and discussion

4.1. Discrete validation

In order to verify the reliability of the simulating model, a large amount of calculations based on different discrete were conducted. The comparison of two sets of grid models is listed in Table 3. The sectional view of computational meshes is shown in Fig. 4. Wherein, one group has 40 sections along the x -direction, 60 sections along the y -direction and 1000 sections along z -direction. For another group, grid sections are set as 50, 70 and 1200 along x -

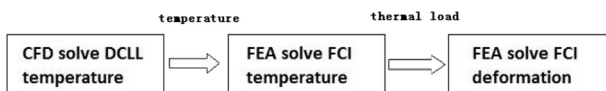


Fig. 3. Work chart for simulating thermo-fluid-structure coupled field.

Table 3
Temperature calculated by different grids.

Grid division	Point (0.085, 0, 2)	Point (0.095, 0, 1.8)	Point (0.099, 0, 1.8)
40 × 60 × 1000	721.393 K	702.548 K	680.094 K
50 × 70 × 1200	721.410 K	702.538 K	680.091 K

direction, y -direction and z -direction, respectively. The flow channel insert, the gap flow area and the steel wall are divided into 8 sections across the thickness direction. As shown in Table 3, calculating results for temperature are very close in these two cases, which implies that the discretion is reasonable.

4.2. Thermal deformation and stress of FCI in temperature field

The temperature distribution on three different sections $z = 0.2$ m, $z = 1.0$ m and $z = 1.8$ m are shown in Fig. 5 (the convection heat coefficient between steel wall and helium is 4000 W/m² K and thermal conductivity of FCI is 15 W/m K, respectively). Because the heat of high temperature fluid in bulk flow is transferred through the FCI and steel wall to external helium continuously with the fluid flowing, the temperature gradually decreases from the centre of bulk flow to outer wall of FW. As the thermal conductivity of SiC is worse than that of metal fluid, the temperature gradient in FCI is greater than that in metal fluid along either radial or toroidal direction.

Fig. 5(a) indicates that the temperature in core region remains almost the same, while the temperature near outside wall decreases along the flow direction. Fig. 5(b) and (c) shows that the temperatures decrease almost linearly through the thickness of FCI. The temperature difference through the thickness of FCI is greater in the inlet area, because the temperature difference between gap flow and Helium is greater and the effect of convection heat transfer is stronger in this zone. Additionally, the temperature gradient in FCI wall decreases gradually along the flow direction.

Fig. 6 shows the deformation of FCI (the deformation has been amplified to be clearly viewed). The effects of high entrance temperature of fluid and restriction of FCI in the inlet end lead to the maximum displacement (about 2.7416 × 10⁻⁵ m) at the corner of FCI (as seen in Fig. 6(a)). Due to convection heat transfer effect, temperature in FCI would be lower along the flow direction, which would result in decrease of thermal deformation of FCI. Fig. 6(b) indicates that the deformation on edges is the greatest and deformation along the line of $x = 0$ m and $y = 0.15$ m is greater than that along the line of $x = 0.1$ m and $y = 0$ m.

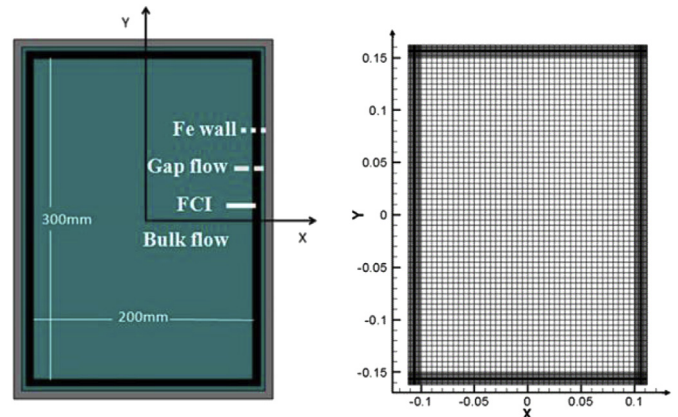


Fig. 4. Section and meshing of DCLL model.

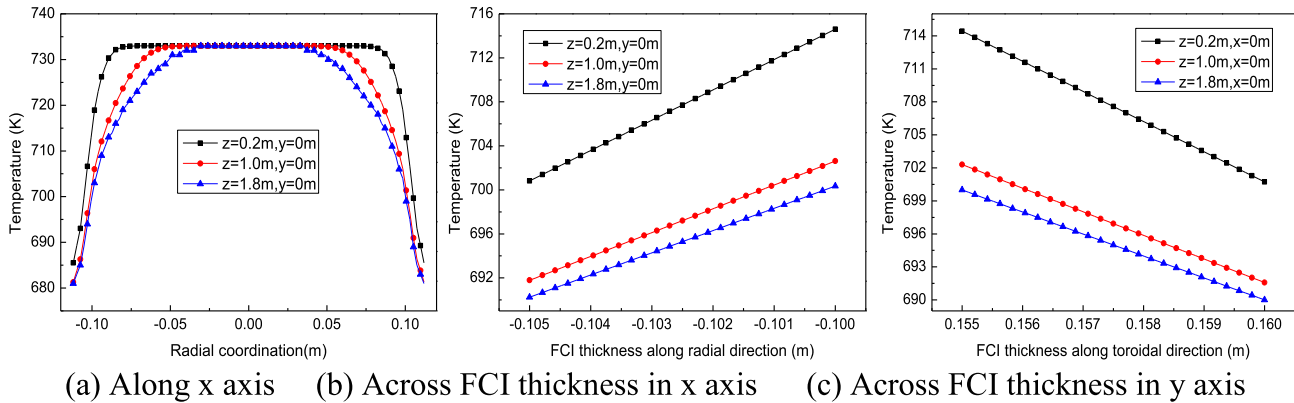


Fig. 5. The temperature distribution at different sections.

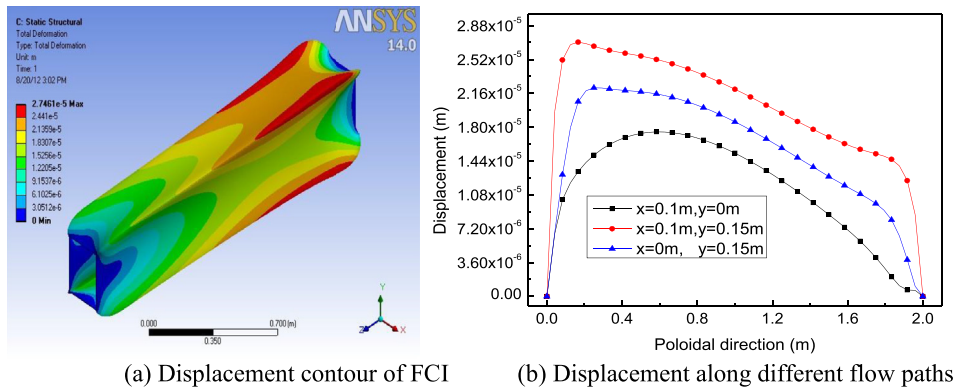


Fig. 6. Thermal displacement of FCI.

Fig. 7 demonstrates the von Mises stress distribution in flow channel insert. The maximum value (275.8 MPa) appears at outer corner near the inlet end of FCI. That is resulted from coupling effects of thermal expansion and displacement restriction on boundary. The Mises stresses in other parts of FCI remain almost the same along the flow direction.

Fig. 8 indicates the deformation and stress variations through the thickness of FCI. The displacement remains almost the same through the thickness of FCI, but has great change along flowing direction. The displacement near inlet end is almost 5.5 times of that at outlet end, as seen in Fig. 8(a).

The curves in Fig. 8(b) show that the stresses on the inner wall of FCI are greater than that on the outer wall because the

temperature of gap flow decrease more rapidly than that of bulk flow for the effect of heat transfer to cold liquid helium. The variation rates of stress near the inlet end are greater. And coupled effects of boundary restriction and temperature field make Mises stresses near both ends of FCI greater than that in the middle of FCI.

4.3. The effects of convection heat transfer

In the DCLL design, helium is an important coolant for the ferritic wall. Heat transfer between ferritic wall and helium greatly influences the thermal stresses and deformation of FCI. In this work, three cases with different heat transfer coefficients (2000 W/

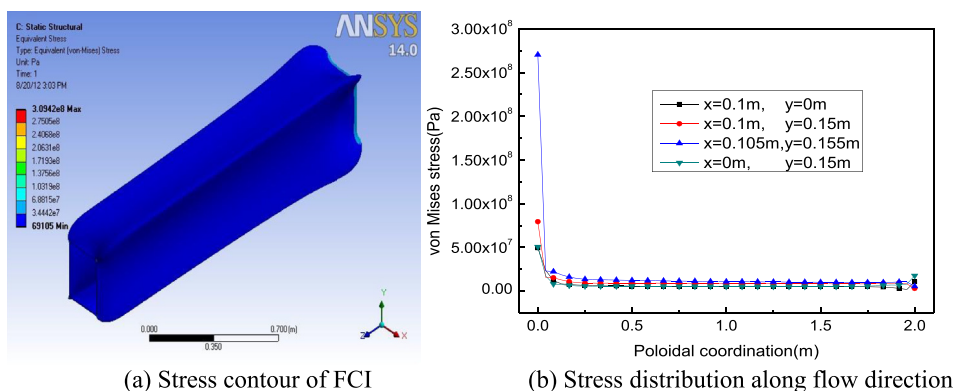


Fig. 7. Thermal stress in FCI.

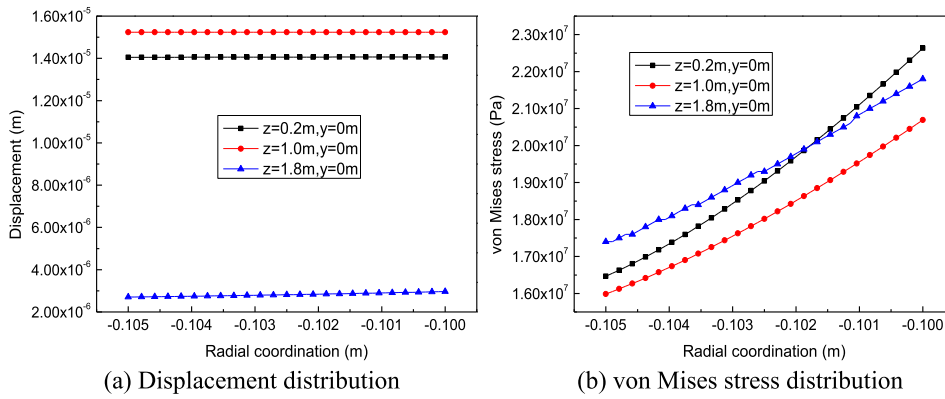


Fig. 8. Deformation and stress through thickness of FCI.

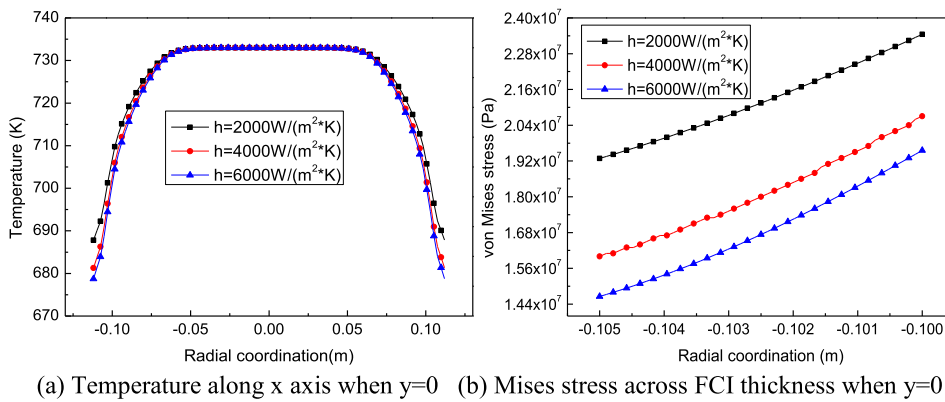


Fig. 9. Influence of convection heat transfer on temperature field and stress field.

$m^2 K$, $4000 W/m^2 K$ and $6000 W/m^2 K$) were simulated to analyze the influence of heat transfer on temperature and stresses of FCI.

The results, as shown in Fig. 9, indicate temperature distribution, deformation and Mises stress. Fig. 9(a) shows that temperatures in bulk flow area are almost the same in three cases. This indicates that convective heat transfer will not affect much in outlet flow temperature since FCI's effect as thermal insulator. Additionally, temperature of FCI itself will decrease since more heat will be transferred by the helium. Despite trivial changes in temperature gradient across FCI thickness (seen in Fig. 9(b)), the thermal deformation and stress will still decrease due to a lower overall temperature in FCI.

Fig. 10(a) and (b) indicates influences of convection heat transfer coefficients on the maximum thermal displacement and von Mises stress of FCI. Both thermal displacement, stress and their gradients reduce with higher heat transfer coefficient. This indicates that a higher convective heat transfer coefficient is beneficial for the FCI structural safety without much affect to the bulk flow temperature.

4.4. The effects of thermal conductivity of FCI

FCI can reduce heat leakage from bulk flow into helium as well as reduce MHD pressure drop. Different manufacturing process can greatly affect physical properties of silicon carbide composite

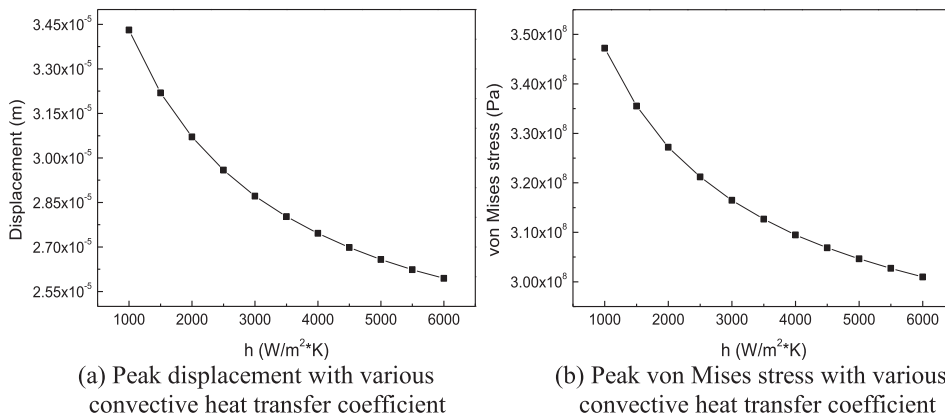


Fig. 10. Influence of convective heat transfer on thermal deformation and von Mises stress.

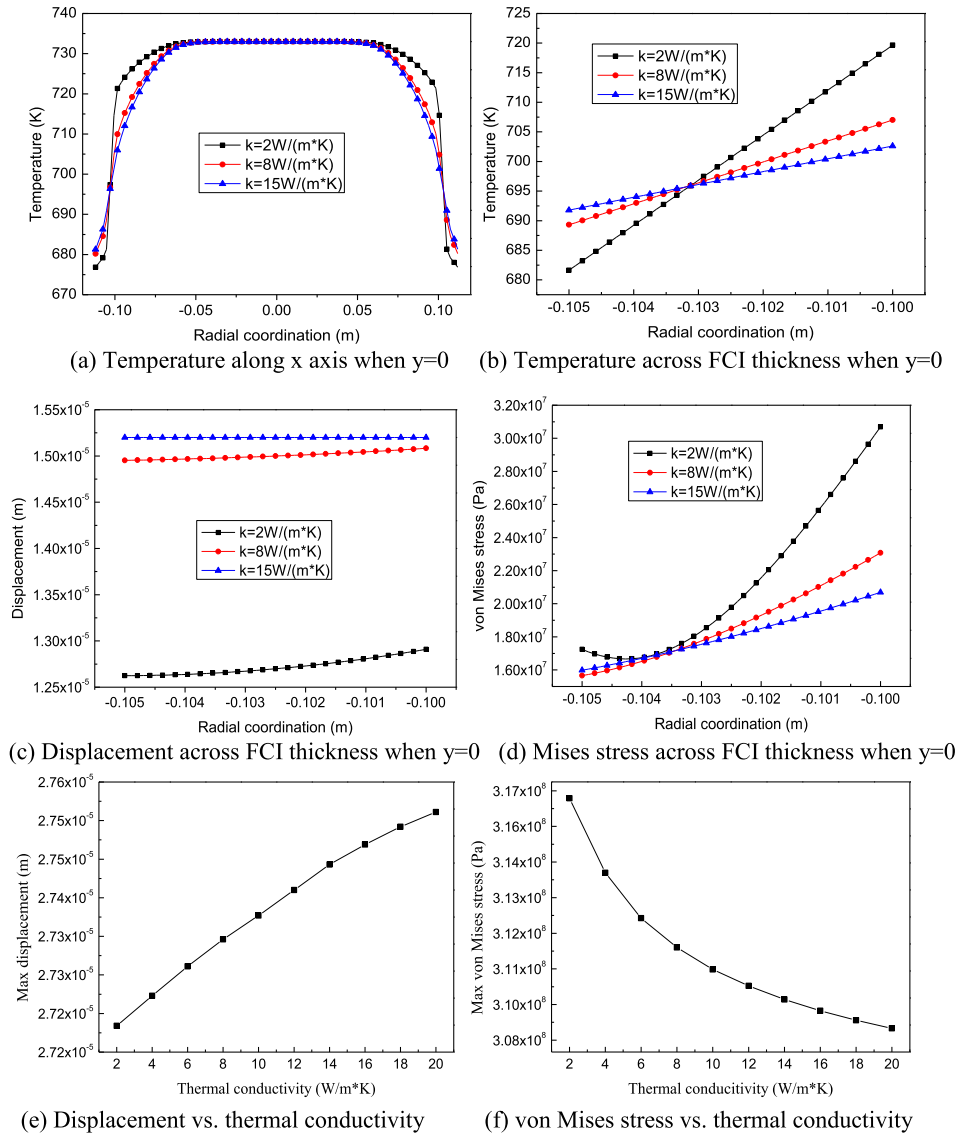


Fig. 11. Effects of thermal conductivity of FCI.

which FCI is made of. Its thermal conductivity can vary from 2 W/m K to 20 W/m K. In order to investigate the effects of FCI thermal conductivity on the blanket module, three cases (thermal conductivity as 2 W/m K, 8 W/m K, and 15 W/m K) were carried out.

Fig. 11(a) indicates that the peak temperature in bulk flow will remain almost the same with larger FCI thermal conductivities. However, temperature in other parts of bulk flow ($-0.10 \text{ m} < x < -0.07 \text{ m}$ and $0.07 \text{ m} < x < 0.10 \text{ m}$) will be lower when FCI has a larger thermal conductivity. This indicates more heat leakage from bulk flow into helium in this case. Thus, average outlet temperature of bulk flow will be lower, and this will lead to lower heat efficiency in the following Brayton cycle.

On the other hand, when FCI has a larger thermal conductivity, temperature gradient across FCI thickness will decrease greatly (seen in Fig. 11(b)). And this will directly affect thermal stresses in FCI (shown in Fig. 11(d)). Interestingly, while thermal conductivity is 2 W/m K, the stress across FCI thickness changes nonlinearly, this is due to the coupling effect of heat transfer effects from both metal flow and helium convection. Fig. 11(c) shows that better heat conductivity leads to larger displacement yet smaller displacement

gradient across the FCI thickness. And as can be seen in Fig. 11(e) and (f), with better thermal conductivity, the maximum thermal displacement increases while the thermal stress decrease. Thus, a better thermal insulated FCI is beneficial for enhancing outlet flow temperature and preventing heat leakage into helium, however, it will increase FCI temperature gradient and thermal stress.

5. Conclusions

In this work, coupled thermal, hydrodynamic and elastic issues in DCLL blanket were studied applying finite element–finite volume method. The effects of flow and heat transfer were taken into account. Temperature distributions in coupled heat transfer effects were obtained. And structural safety of FCI was investigated in detail. Results lead to following conclusions.

- (1) Stress concentration appears at the two ends of FCI, this is due to the coupling effect of thermal expansion and displacement constraint. FCI corners near the high temperature inlet end are the most dangerous area. Thermal stresses

should be prioritized in FCI structural safety since pressure effect would lead to negligible stresses comparing with thermal stress.

- (2) Higher heat transfer coefficient will reduce the overall FCI temperature and its thermal stress. This is beneficial for the FCI structural safety without affecting the bulk flow temperature much.
- (3) Smaller FCI thermal conductivity is beneficial for preventing heat leakage into helium, enhancing outlet flow temperature as well as raising heat efficiency. However, it will greatly increase FCI temperature gradient and thermal stress. Structural safety of FCI shall be concerned in this case.

Conclusions above can provide supports for design and optimisation of the blanket module. Further researches on coupling dynamics behaviour of FSI with heat transfer effect should be expected.

Acknowledgement

This work was financially supported by the National Natural Science Foundation of China (No. 51376175), and the ITER major project from the National Basic Research Program of China (973 program, No. 2013GB114001).

References

- [1] M. Abdou, et al., U.S. plans and strategy for ITER blanket testing, *Fusion Sci. Technol.* 47 (3) (2005) 475–487.
- [2] A. Raffray, R. Jones, et al., Design and material issues for high performance SiC_f/SiC-based fusion power cores, *Fusion Eng. Des.* 55 (1) (2001) 55–95.
- [3] H. Yu, X. Zhou, et al., 2D SiC_f/SiC composite for flow channel insert (FCI) application, *Fusion Eng. Des.* 85 (2010) 1693–1696.
- [4] S. Ueda, et al., A fusion power reactor concept using SiC_f/SiC composites, *J. Nucl. Mater.* 258 (1998) 1589–1593.
- [5] S. Smolentsev, N.B. Morley, M. Abdou, Code development for analysis of MHD pressure drop reduction in a liquid metal blanket using insulation technique based on a fully develop flow model, *Fusion Eng. Des.* 73 (2005) 83–93.
- [6] S. Smolentsev, N.B. Morley, M. Abdou, Magnetohydrodynamic and thermal issues of the SiC_f/SiC flow channel insert, *Fusion Sci. Technol.* 50 (2006) 107–119.
- [7] S. Smolentsev, et al., Numerical analysis of MHD flow and heat transfer in a poloidal channel of the DCLL blanket with a SiC_f/SiC flow channel insert, *Fusion Eng. Des.* 81 (2006) 549–553.
- [8] Z. Xu, C. Pan, W. Wei, Experimental investigation and theoretical analysis two dimensional MHD effects in rectangular duct, *Fusion Technol.* 36 (1) (1999) 47–51.
- [9] Z. Xu, C. Pan, X. Zhang, L. Zhao, J. Zhang, G. Yang, Primary experimental results of MHD flow in the duct with flow channel insert, *Nucl. Fusion Plasma Phys.* 29 (2009) 6–9.
- [10] W. Wang, FSD Team, et al., Three dimension numerical analysis of flow and heat transfer for Chinese liquid metal LiPb experimental loop dragon, *Chin. J. Nucl. Sci. Eng.* 30 (2010) 166–171.
- [11] Y. Wu, FSD Team, Design analysis of China dual-functional lithium lead (DFLL) test blanket module in ITER, *Fusion Eng. Des.* 82 (2007) 1893–1903.
- [12] Y. Katoh, S. Kondo, L.L. Snead, DC electrical conductivity of silicon carbide ceramics and composites for flow channel insert applications, *J. Nucl. Mater.* 386 (2009) 639–642.
- [13] M. Ni, J. Li, A consistent and conservative scheme for incompressible MHD flows at a low magnetic Reynolds number. Part III: on a staggered mesh, *J. Comput. Phys.* 231 (2) (2012) 281–298.